THE JOURNAL OF PHYSICAL CHEMISTRY C

Article

Cite This: J. Phys. Chem. C 2019, 123, 21571−21580

pubs.acs.org/JPCC

# Comparative Study of the Adsorption of Thiol and Isocyanide Molecules on a Silver Surface by in Situ Surface-Enhanced Raman Scattering

*Published as part of The Journal of Physical Chemistry virtual special issue "Hai-Lung Dai Festschrift".*

Jaewan Ahn, Shi Shi, Bonnie Vannatter, and Dong Qin*

School of Materials Science and Engineering, Georgia Institute of Technology, Atlanta, Georgia 30332, United States

Supporting Information

**ABSTRACT:** We report an investigation of the adsorption of thiol and isocyanide molecules on colloidal Ag nanocubes through surface-enhanced Raman scattering (SERS). Specifically, we collect SERS spectra in situ at different time points from a mixture of Ag nanocubes and ligand molecules at a specific concentration. We demonstrate that 4-nitrothiophenol could readily bind to the Ag surface through strong thiol−Ag interaction. We also observe red shifts for the SERS peaks as the concentration decreases, suggesting a change to the molecular orientation relative to the surface. Likewise, 4-aminothiophenol also adsorbs onto Ag quickly, but gives much weaker SERS signals relative to 4-nitrothiophenol because the electron-donating amine group would retard the chemical enhancement of SERS. Different from thiols, 1,4-phenylene diisocyanide binds to Ag surface through a relatively weak, $\sigma$-donation bond. With an increase in concentration, molecules tend to adsorb on the nanocubes with the benzene ring tilting away from the surface. We further investigate the competitive binding of thiol and isocyanide, demonstrating the capability of thiol to inhibit the adsorption of isocyanide when these two ligands are presented in a mixture.

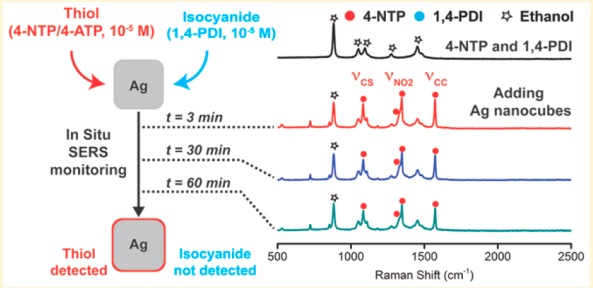


## INTRODUCTION

The surface of metal nanoparticles is prone to the adsorption of organic molecules because the adsorbates can reduce the interfacial energy between the metal and its surrounding medium.[1] If the organic molecules have a functional group with strong affinity toward the metal atom, they tend to spontaneously arrange themselves into a self-assembled monolayer (SAM),[2] presenting a robust method for engineering the interfacial properties.[3−6] Although there are extensive reports on the formation of thiol-based SAMs on Au nanoparticles,[2,7−10] it remains challenging to characterize the surface adsorption process in gathering information such as coverage density, conformation of the adsorbed ligands, and the relative binding strengths of different ligands. To this end, it is of importance to develop a technique capable of probing the adsorption of organic molecules on the surface of nanoparticles in situ. Such a technique would also find immediate use in areas such as surface science and heterogeneous catalysis.

There are a number of documented techniques for characterizing the adsorption of organic molecules on a solid surface. As a direct method, scanning tunneling microscopy (STM) has been used extensively to visualize the SAM on a metal thin film by obtaining topological information with resolution down to the molecular level.[11,12] Recent reports suggested that STM could analyze mixed-ligand SAMs on Au nanoparticles with sufficient sensitivity to distinguish between the regions comprised of different types of thiol molecules.[13,14] Unfortunately, STM measurements demand a high-vacuum environment,[15] making it impractical to gather information from a solution-phase system. Additionally, it is difficult to extract configuration of organic molecules on a solid surface from the STM data. In comparison, other indirect methods can reveal the structural details of the adsorbed molecules by leveraging molecular vibrations. Among them, Fourier-transform infrared spectroscopy (FTIR) is well-known for its ability to reveal the molecular fingerprints about the adsorbates. For example, Murray et al. demonstrated the use of FTIR to evaluate the conformations of alkanethiol molecules adsorbed on Au nanoparticles as a function of particle size and under different conditions (e.g., solid state vs solution phase).[16,17] They discovered that alkanethiols would show less ordered packing on smaller particles or for the nanoparticles dispersed in nonpolar solvents. On the basis of the nonlinear optical responses from the surface of nanoparticles,[18,19] second-harmonic generation (SHG) spectroscopy serves as a sensitive technique to create the adsorption isotherm,[20] to determine the adsorption energy and coverage density,[21] and to

Received: June 5, 2019
Revised: August 12, 2019
Published: August 13, 2019







DOI: 10.1021/acs.jpcc.9b05383
J. Phys. Chem. C 2019, 123, 21571−21580

investigate the exchange of different ligands on the surface of Au nanoparticles.[22] However, SHG inherits a number of intrinsic problems, including bulk-phase interference, sensitivity restriction, limited range of wavenumbers, and an inability to detect vibrational modes parallel to the interfacial plane as a result of surface-selection rules.

Surface-enhanced Raman scattering (SERS) offers a powerful tool for analyzing molecular adsorption on the surface of a plasmonically active metal such as Au or Ag in liquid phase and under ambient conditions. SERS shares several attributes with electron energy loss spectroscopy (EELS), including the excellent sensitivity toward low wavenumbers and the ability to detect most adsorbate through their vibrational modes. In the 1990s, Weaver and others used SERS to study the interface between an aqueous phase and an electrocatalytic material that includes a roughened noble-metal electrode or an electrode decorated with nanoparticles of 1−2 nm in size.[23−27] They argued about the feasibility to monitor molecular transformations on a catalytic surface by following the vibrational fingerprints of catalytically relevant molecules, such as ethylene, methanol, and carbon monoxide, as a function of electrode potential.[23−25] In recent years, SERS has been implemented to probe chemical reactions in situ on nanoparticles consisting of a plasmonic metal such as Au or Ag and a catalytic metal such a Pd or Pt.[28−30] Most recently, we further demonstrated the utility of SERS in probing the heterogeneous nucleation and growth of Pd or Pt on Ag nanocubes in solution with the introduction of an isocyanide probe.[31,32] Despite these prior reports, SERS has not been fully explored for in situ monitoring of the adsorption of an organic ligand onto the surface of metal nanocrystals in a solution phase.[33−35]

Herein, we demonstrate the use of SERS as a platform technique to investigate the competitive adsorption of thiol and isocyanide molecules on the surface of Ag nanocubes. As illustrated in Figure 1, we selected three different ligands, 4-nitrothiophenol (4-NTP), 4-aminothiophenol (4-ATP), and 1,4-phenylene diisocyanide (1,4-PDI), to investigate their (competitive) adsorption on the surface of Ag nanocubes. It is well-known that both 4-NTP and 4-ATP can chemisorb onto Ag via the establishment of a Ag−thiolate linkage.[36,37] Since $-NO_2$ and $-NH_2$ are an electron acceptor and a donor, respectively, 4-NTP and 4-ATP have been used to study the role of charge transfer in affecting the SERS activities of Ag nanoparticles.[38,39] A number of groups have also investigated the production of an azo-compound from 4-NTP or 4-ATP on the surface of Ag or Au nanoparticles using SERS.[39−41] Different from thiol molecules whose vibrational modes exhibit essentially no dependence on the metal surface, the binding of the isocyanide group (−NC) to a transition metal is similar to that of carbon monoxide, making the stretching frequency of the NC bond ($\nu_{NC}$) sensitive to the interaction between the −NC group and the metal.[42−45] The carbon is assumed to bind to Ag through $\sigma$-donation, by which the lone-pair electrons are donated from the antibonding $\sigma^*$ orbital of the −NC group to the d-band of Ag. It is anticipated that there are two possible configurations of 1,4-PDI on the surface of Ag nanocubes. The first configuration involves the binding of one −NC group to Ag in a standing geometry with respect to the surface while leaving the other −NC group free.[46] The second one reflects the binding of both −NC groups to the Ag surface. Because the $\nu_{NC(Ag)}$ and $\nu_{NC(free)}$ peaks have distinctive Raman shifts, it is feasible to characterize the configuration of 1,4-PDI on the surface of Ag by SERS. It is worth acknowledging that isocyanides have received attention in the molecular electronics community due to the lower barrier to electron transfer at the isocyanide−metal junction than that at the thiol−metal junction.[47,48] It has been argued that 1,4-PDI could serve as a molecular linker to bridge two metal electrodes through the two −NC groups and $\pi$-conjugated benzene ring to achieve efficient electron transfer.[48]

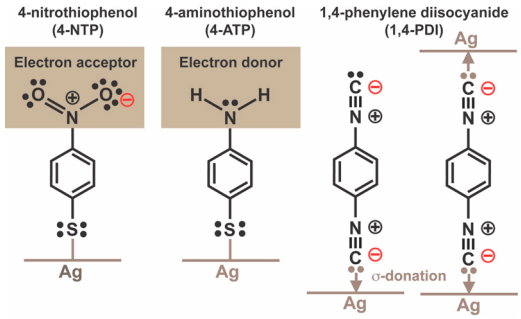


**Figure 1.** Molecular structures of the ligands and schematic illustrations showing how these ligand molecules bind to the surface of Ag nanocubes.

In this work, we investigate the adsorption of 4-NTP, 4-ATP, and 1,4-PDI on the surface of colloidal Ag nanocubes suspended in ethanol by in situ SERS. In a typical process, we disperse the acid-treated Ag nanocubes in an ethanol solution containing either 4-NTP, 4-ATP, or 1,4-PDI, followed by the collection of SERS spectra at different time points. Because the SERS hot spots are located on the edges of Ag nanocubes, we actually monitored the adsorption of thiol or isocyanide on the edges. By varying the concentration of each solution, there are some subtle differences in the vibrational peaks from the SERS spectra, suggesting that the configurations of molecules on the Ag surface likely change when the surface coverage of ligand molecules was altered. More interestingly, we further evaluate competitive adsorption of thiol and isocyanide by dispersing Ag nanocubes in an ethanol solution containing both thiol (4-NTP or 4-ATP) and 1,4-PDI. Our results confirm the preference of thiol over isocyanide in adsorbing onto Ag surface when these two ligands are presented in comparable concentrations.

## EXPERIMENTAL SECTION

**Chemicals.** Ethylene glycol (EG) was purchased from J. T. Baker (Avantor Performance Materials, LLC, Center Valley, PA). Silver trifluoroacetate ($CF_3COOAg$, ≥ 99.99%), sodium hydrosulfide hydrate ($NaHS{\cdot}xH_2O$), poly(vinylpyrrolidone) (PVP) with an average molecular weight of 29 000 (PVP-29), aqueous hydrochloric acid (HCl, 37 wt %), L-ascorbic acid ($H_2Asc$, 99%), ethyl alcohol (ethanol, ≥ 99.5%), 1,4-phenylene diisocyanide (1,4-PDI, 97%), 4-nitrothiophenol (4-NTP, 80%), and 4-aminothiophenol (4-ATP, 97%) were ordered from Sigma-Aldrich (St. Louis, MO). Acetone (≥99.5%) was purchased from Alfa Aesar (Haverhill, MA). All chemicals were used as received. Deionized (DI) water with a resistivity of 18.2 MΩ·cm at room temperature was obtained from the EMD Millipore Direct-Q 3UV ultrapure water purification system (MilliporeSigma, Burlington, MA).

**Synthesis of Ag Nanocubes.** We followed a published protocol involving polyol reduction to synthesize the Ag



DOI: 10.1021/acs.jpcc.9b05383
J. Phys. Chem. C 2019, 123, 21571−21580

nanocubes.[49] The as-prepared Ag nanocubes were washed once with acetone, followed by three times with water, and then dispersed in water for storage and future use. The stock suspension of Ag nanocubes contained $1.2 \times 10^{13}$ particles per mL.

**Acid Treatment of Ag Nanocubes.** In a standard protocol, we mixed 0.5 mL of aqueous $H_2Asc$ (0.1 M) and 2 mL of aqueous PVP-29k (1 mM) in 0.5 mL of water in a 23 mL glass vial under magnetic stirring at 650 rpm. Next, we injected 25 $\mu$L of Ag nanocubes to the acidic solution to attain approximately $3.0 \times 10^{11}$ particles. The mixture was magnetically stirred under ambient conditions for 2 h. Afterward, the solution was divided and transferred into three centrifuge tubes, followed by their centrifugation at 5500 rpm for 15 min. After the removal of the supernatant, the solids were used without further modification for the SERS experiments. For TEM characterization, the solids were washed with ethanol twice and drop-casted onto a TEM grid.

**Monitoring the Adsorption of 4-NTP, 4-ATP, or 1,4-PDI on Ag Nanocubes by SERS.** In a standard protocol, we first recorded a Raman spectrum from the ligand, such as 4-NTP, 4-ATP, or 1,4-PDI in ethanol solution at the concentration of $10^{-5}$ M, as a reference. Next, we mixed the ligand solution with the Ag nanocubes, followed by rigorous shaking to disperse the nanocubes. Finally, we withdrew aliquots from each sample at 3, 15, 30, 45, 60 min for SERS measurements. For the experiments involving different concentrations of ligand, we followed the standard protocol except that the ligand solution was changed to either $10^{-4}$ or $10^{-7}$ M.

**Monitoring the Competitive Adsorption of 1,4-PDI and 4-NTP, as well as 1,4-PDI and 4-ATP, on Ag Nanocubes by SERS.** In a typical experiment, we mixed two ligand solutions (4-NTP and 1,4-PDI or 4-ATP and 1,4-PDI), each at a doubled concentration (that is, $2 \times 10^{-3}$, $2 \times 10^{-5}$, or $2 \times 10^{-7}$ M) relative to the standard protocol, in equal volumes. As a result, the final mixture would preserve the concentrations of each ligand relative to the single-ligand experiments. We then followed the standard protocol except that the mixture was used as the ligand solution.

**Raman Measurements.** We performed our Raman measurements using a Renishaw inVia Raman spectrometer (Wotton-under-Edge, U.K.) coupled with a Leica optical microscope (Leica Camera, Wetzlar, Germany). In a typical measurement, we transferred an aliquot of 20 $\mu$L from the sample into a transparent polydimethylsiloxane (PDMS) cell, covered the cell with a thin cover glass, and placed the cell on the sample stage of microscope. After we used the *static* mode for collecting consecutive Raman spectra every second to confirm that the Raman signal was relatively stable (variation is within 100 counts), we recorded the Raman spectrum in the *extended* mode, using the excitation wavelength of 532 nm, 100× objective, 10% of the laser power (maximum power of 50 mW), and 10 s collection time.

**Quantitative Analysis of Raman Data.** We used Renishaw's WiRE 5.1 software to calculate the area under the peaks of the characteristic Raman bands present in the SERS spectra at each time point in the experiment, specifically the $\nu_{CC}$ band of 4-NTP and the $\nu_{NC(Ag)}$ band of 1,4-PDI. For each data point, we performed the analysis according to the following procedure. In the first step, we loaded the raw data into the software and then centered the viewing window around the peak of interest (1520−1620 $cm^{-1}$ for the $\nu_{CC}$ band, and 2000−2300 $cm^{-1}$ for the $\nu_{NC}$ band). In the second step, based on the curve-fitting function in the software, we attempted to fit the data using a single Gaussian—Lorentzian peak (50% of each character). The software optimized the curve fit model to minimize the sum of the squared deviations of the fitting from the experimental data, updating the information such as the peak center, peak width, peak height, and the shape (proportion of the Gaussian character). If we could not fit the band, we would add a second peak and perform the optimization again to better capture the peak area of this band. Finally, we took the sum of the peak areas of all curves used in this fitting to obtain the total area under the peak.

**Instrumentation and Characterization.** The nanoparticles were collected using an Eppendorf 5430 centrifuge (Eppendorf North America, Hauppauge, NY). The pH values were measured using a FiveEasy pH Meter (Mettler Toledo, Columbus, OH). The UV−vis spectra were collected using the Cary 60 spectrophotometer (Agilent Technologies, Santa Clara, CA). Transmission electron microscopy (TEM) images were captured on a Hitachi HT7700 microscope (Tokyo, Japan) operated at 120 kV.

## RESULTS AND DISCUSSION

We prepared Ag nanocubes by following the protocol published by Xia and co-workers.[49] To remove any oxides on the surface, we dispersed the Ag nanocubes in an acidic solution (pH = 3.1) containing $H_2Asc$ and PVP under magnetic stirring for 120 min. Figure S1 shows TEM images of the samples before and after acid treatment, indicating no significant changes to the morphology of nanocubes. After collecting the acid-treated Ag nanocubes via centrifugation, we immediately redispersed them in an ethanol solution containing the ligand molecules, followed by withdrawing aliquots from each sample at various time points for SERS measurements. In this study, we assume that the primary contribution to SERS signals would come from molecules adsorbed on the edges of individual Ag nanocubes where hot spots are located, rather than from those situated in the interparticle junctions.[31] To validate our hypothesis, we recorded UV−vis spectra from the Ag nanocubes dispersed in the acid solution and the acid-treated nanocubes redispersed in the ethanol solution. As shown in Figure S2, there was essentially no change to the UV−vis spectra, confirming the absence of aggregation for the acid-treated Ag nanocubes redispersed in the ethanol solution. It is also worth mentioning that we could use the Raman peak of ethanol at 879 $cm^{-1}$ as an internal reference to calibrate the Raman system. As confirmed by the spectra in Figure S3, this band remained at essentially the same position before and after the introduction of Ag nanocubes.

We initially studied the interaction of thiols with Ag nanocubes by employing 4-NTP as the ligand. Figure 2A shows Raman spectra collected from a 4-NTP solution ($10^{-5}$ M) in ethanol before and after adding the acid-treated Ag nanocubes. On the basis of our back-of-the-envelope calculation, it is reasonable to assume that the 4-NTP molecules at this concentration would be able to form a full coverage on the Ag nanocubes. In the absence of Ag nanocubes, the Raman spectrum only shows the peaks associated with ethanol. At $t$ = 3 min after the introduction of nanocubes, the characteristic peaks of 4-NTP appeared at 1083 (C−S stretching, $\nu_{CS}$), 1336, 1347 ($NO_2$ stretching,


DOI: 10.1021/acs.jpcc.9b05383
J. Phys. Chem. C 2019, 123, 21571−21580

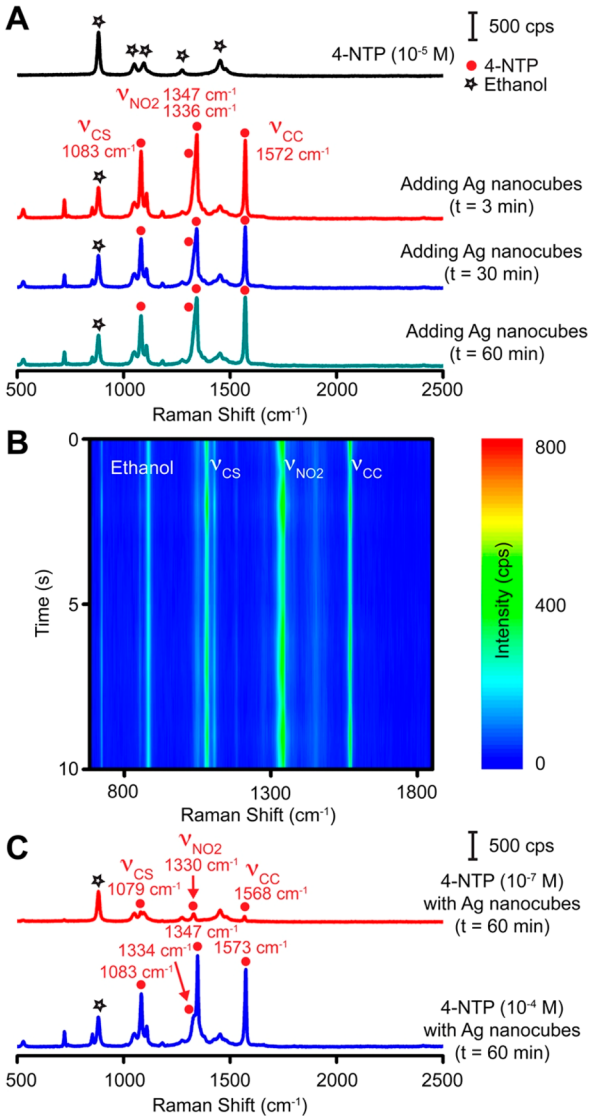


**Figure 2.** (A) Raman spectrum of 4-NTP ethanol solution ($10^{-5}$ M) and the SERS spectra of 4-NTP collected from the same solution at different time points after the introduction of Ag nanocubes. (B) Time-dependent SERS spectra of 4-NTP collected at 3 min. (C) SERS spectra of 4-NTP collected at $t$ = 60 min after introducing Ag nanocubes into the 4-NTP ethanol solutions at concentrations of $10^{-7}$ M and $10^{-4}$ M, respectively.

$\nu_{NO_2}$), and 1572 cm$^{-1}$ (C−C stretching, $\nu_{CC}$). The frequencies and intensities of these peaks did not change over a period up to $t$ = 60 min. It is worth mentioning that we calibrated our Raman spectrometer using Si(100) as a reference every time before we performed SERS measurements. On the basis of 20 calibrations, Table S1 shows that the spectrometer consistently gives the Raman shift of Si(100) at 520.29 cm$^{-1}$ with a standard deviation of 0.09 cm$^{-1}$. With regard to the peak intensity, Figure 2B shows the time-dependent SERS spectra (in the form of a heat map) of 4-NTP collected 3 min after the introduction of Ag nanocubes into $10^{-5}$ M 4-NTP ethanol solution, suggesting that the SERS signal remains stable during the collection time of 10 s. It is interesting to note that the stretching mode of $NO_2$ ($\nu_{NO_2}$) was split into two peaks at 1336 and 1347 cm$^{-1}$. Although this observation is different from those reported in previous ex situ SERS experiments involving 4-NTP,[41,50] we are still unable to fully elucidate the nature of these two peaks at the moment.

By varying the concentration of 4-NTP while keeping the number of Ag nanocubes unchanged in the ethanol solution, we investigated how the molecules would interact with the Ag surface differently. At $t$ = 60 min, Figure 2C shows the SERS spectra of 4-NTP adsorbed onto the Ag nanocubes from solutions with concentrations at $10^{-7}$ and $10^{-4}$ M, respectively. At $10^{-7}$ M, we noticed that the Raman peaks of 4-NTP were noticeably red-shifted to 1079 ($\nu_{CS}$), 1330 ($\nu_{NO_2}$), and 1568 cm$^{-1}$ ($\nu_{CC}$), respectively, while the other $\nu_{NO_2}$ peak at 1346 cm$^{-1}$ was missing. Based on peak areas of $\nu_{NO_2}$, the SERS signal became 20-fold weaker relative to that of $10^{-5}$ M. Conversely, at $10^{-4}$ M, the peaks of 4-NTP appeared at 1083 ($\nu_{CS}$), 1334, 1347 ($\nu_{NO_2}$), and 1573 cm$^{-1}$ ($\nu_{CC}$), consistent with the peak positions at $10^{-5}$ M. Also, the peak intensities were comparable to those shown in Figure 2A.

To further evaluate the concentration-dependent adsorption of 4-NTP on Ag nanocubes, we performed SERS measurements three times at concentrations of $10^{-7}$, $10^{-5}$, or $10^{-4}$ M, respectively. By fitting the $\nu_{cc}$ band (see details in the Experimental Section), Figure 3 shows three plots of the peak area as a function of time at three concentrations. Our data suggest that the SERS signal reached a stable state within 3 min regardless of the concentration of 4-NTP, suggesting that the adsorption of 4-NTP on the surface of Ag nanocubes

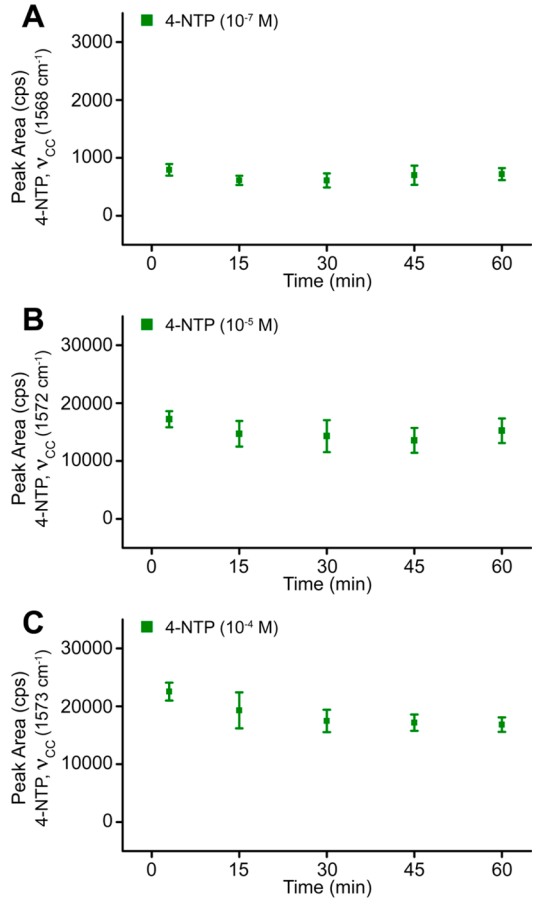


**Figure 3.** Plots of peak area for the $\nu_{CC}$ band of 4-NTP as a function of time at the concentration of (A) $10^{-7}$, (B) $10^{-5}$, and (C) $10^{-4}$ M, respectively.



DOI: 10.1021/acs.jpcc.9b05383
J. Phys. Chem. C 2019, 123, 21571−21580

could reach equilibrium at a time scale less than 3 min. Because the SERS hot spots are located on the 12 edges of a Ag nanocube while the cube is predominantly enclosed by six side faces, it is not surprising to resolve much weak SERS signal at a concentration of $10^{-7}$ M when only a limited number of molecules occupied the edges of nanocubes. In comparison, when the concentration was increased to $10^{-5}$ and then to $10^{-4}$ M, the SERS signals became stronger and reached saturation, suggesting that the molecules could fully cover the edges of Ag nanocubes where the SERS hot spots were located. On the other hand, the difference in Raman shifts of 4-NTP at various concentrations may suggest that the 4-NTP molecules could adsorb on the surface of Ag nanocubes in different configurations. It has been established that the orientation of the adsorbed thiols on a metal surface is dependent on the packing density and thus the concentration of the ligand molecules.[2] For example, alkanethiols have been reported to assume an orientation parallel to the metal surface when used at low concentrations, while taking a more or less perpendicular orientation at relatively high concentrations.[51−53] From this perspective, it is possible that the red-shifted SERS peaks observed for 4-NTP at $10^{-7}$ M reflects those of parallel-lying molecules at a low packing density, whereas the peaks of 4-NTP at $10^{-5}$ or $10^{-4}$ M correspond to those perpendicular to the surface in a closely packed monolayer.

We then examined the interaction of 4-ATP with Ag nanocubes. When the electron-withdrawing nitro group is substituted by an electron-donating amine group, we would expect a change to the direction of electron flow between the Ag surface and the molecule, leading to a diminish of chemical enhancement for the SERS.[39] Figure 4A shows the SERS data collected from the acid-treated Ag nanocubes after being redispersed in the 4-ATP ethanol solution ($10^{-5}$ M). At $t$ = 3 min, the characteristic peaks of 4-ATP appeared at 1080 (C−S stretching, $\nu_{CS}$) and 1593 $cm^{-1}$ (C−C stretching, $\nu_{CC}$). These two peaks did not change their positions and intensities up to $t$ = 60 min, consistent with the behavior of 4-NTP. As anticipated, when the ligands were used at the same concentration of $10^{-5}$ M, the intensities of the 4-ATP signals were much weaker than those from 4-NTP (Figure 2A). This trend supports our argument that the signals from 4-ATP should be weaker due to the lack of chemical enhancement. As shown in Figure 4B, we could hardly resolve any peaks associated with 4-ATP at $10^{-7}$ M while the two peaks located at 1080 ($\nu_{CS}$) and 1594 $cm^{-1}$ ($\nu_{CC}$) returned at $10^{-4}$ M at the time point of 60 min.

Different from thiols that form a relatively strong Ag−S bond with the Ag surface, 1,4-PDI weakly binds to the surface of Ag nanocubes through $\sigma$-donation.[44,46] Figure 5A shows

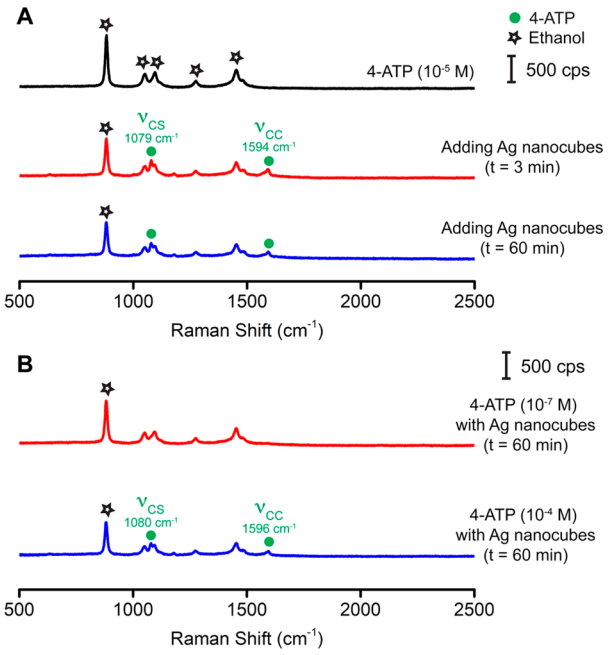


**Figure 4.** (A) Raman spectrum of 4-ATP ethanol solution ($10^{-5}$ M) and SERS spectra of 4-ATP collected from the same solution at different time points after the introduction of Ag nanocubes. (B) SERS spectra of 4-ATP collected at $t$ = 60 min after introducing Ag nanocubes into the 4-ATP ethanol solutions at concentrations of $10^{-7}$ and $10^{-4}$ M, respectively.

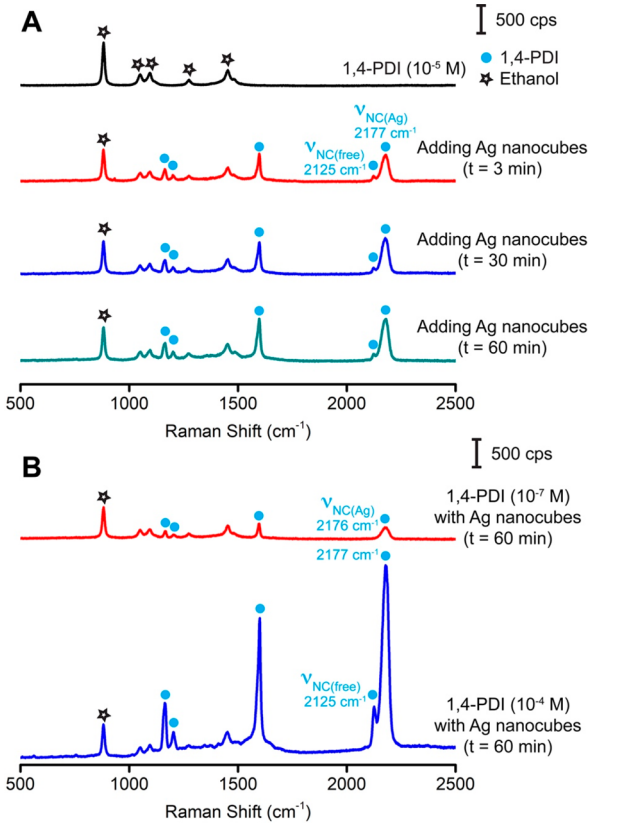


**Figure 5.** (A) Raman spectrum of 1,4-PDI ethanol solution ($10^{-5}$ M) and SERS spectra of 1,4-PDI collected from the same solution at different time points after the introduction of Ag nanocubes. (B) SERS spectra of 1,4-PDI collected at $t$ = 60 min after adding Ag nanocubes into the 1,4-PDI ethanol solutions at $10^{-7}$ and $10^{-4}$ M, respectively.

Raman spectra collected from a 1,4-PDI solution ($10^{-5}$ M) in ethanol before and after adding the acid-treated Ag nanocubes. At $t$ = 3 min, the characteristic peaks of 1,4-PDI emerged at 1164 (C−H bending, $\delta_{CH}$), 1204 (C−NC stretching, $\nu_{C-NC}$), and 1597 (C−C stretching, $\nu_{CC}$), 2125 (N−C stretching, $\nu_{NC(free)}$) and 2177 $cm^{-1}$ (N−C stretching, $\nu_{NC(Ag)}$). At $t$ = 30 min, there was a slight increase in peak intensity. The SERS spectrum then shows little change up to $t$ = 60 min. It is interesting to note that the N−C stretching mode appeared at



DOI: 10.1021/acs.jpcc.9b05383
J. Phys. Chem. C 2019, 123, 21571−21580

2177 and 2125 $cm^{-1}$ in the SERS spectrum with their assignments to the $\nu_{NC(Ag)}$ and $\nu_{NC(free)}$, respectively.[46] The presence of the $\nu_{NC(free)}$ peak suggests that the 1,4-PDI molecules would bind to the surface of the Ag nanocubes through one of its two isocyanide groups only, with the benzene ring tilting away from the surface. We also collected SERS spectra of acid-treated Ag nanocubes after they had been incubated with 1,4-PDI solutions of $10^{-7}$ and $10^{-4}$ M, respectively, at the time point of 60 min. As shown in Figure 5B, at $10^{-7}$ M, the $\nu_{NC(free)}$ peak was not identified while the $\nu_{NC(Ag)}$ peak remained almost unchanged at 2176 $cm^{-1}$. In comparison, at $10^{-4}$ M, we resolved both the $\nu_{NC(Ag)}$ and $\nu_{NC(free)}$ peaks. Based on the peak areas of $\nu_{NC(Ag)}$, the overall SERS signal is about 2-fold weaker at $10^{-7}$ M or 4-fold stronger at $10^{-4}$ M compared with that of $10^{-5}$ M.

To confirm the orientation of 1,4-PDI on Ag surface, we monitored the $\nu_{CH}$ band located at 3065 $cm^{-1}$. According to the surface selection rule, this band can only be identified when the benzene ring is tilting away from the surface.[53] Figure 6A shows a small $\nu_{CH}$ band when Ag nanocubes were functionalized with 1,4-PDI of $10^{-4}$ M. Interestingly, Figure 6B exhibits the appearance of the $\nu_{CH}$ band when we functionalized 1,4-PDI functionalized Ag nanocubes with $10^{-5}$ M and then doubled the number of functionalized cubes used in the standard protocol for SERS measurements. These results support our previous argument that the 1,4-PDI molecules would bind to Ag through a single isocyanide group with the benzene ring tilting away from the surface, giving rise of the $\nu_{NC(free)}$ peak at these two concentrations (see Figure 5, parts A and B). When we functionalized Ag nanocubes with 1,4-PDI of $10^{-7}$ M, followed by SERS detection by increasing the number of Ag nanocubes that are four times larger than those used in the standard protocol to improve detection sensitivity, Figure 6C shows no observation of the $\nu_{CH}$ band even though the increase in the number of nanocubes for this set of SERS measurements was able to increase the peak intensity of $\nu_{NC(Ag)}$ band significantly to the signal level comparable to that of $\nu_{NC(Ag)}$ band collected from Ag nanocubes functionalized with 1,4-PDI of $10^{-5}$ M. Figure S4 shows the direct comparison of the $\nu_{NC(Ag)}$ band, from which one still cannot resolve the $\nu_{NC(free)}$ band. Altogether, we believe that a larger proportion of the 1,4-PDI molecules would bind to the edges of Ag nanocubes, the SERS hot spots, through a single isocyanide group, likely in a benzene ring tilting away from the surface, at a high concentration for accommodating closely packed configuration. In the case of $10^{-7}$ M, it is possible that the molecules might bind to the Ag surface through both isocyanide groups rather than only one of them at such low concentration.

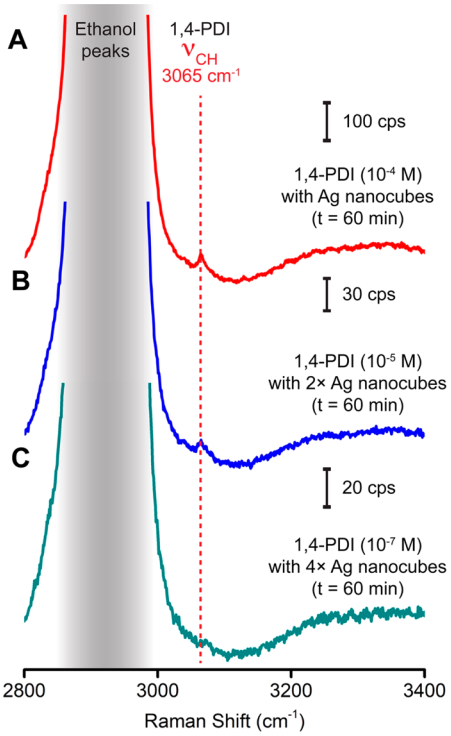


**Figure 6.** SERS spectra of 1,4-PDI collected at $t$ = 60 min by using (A) Ag nanocubes prepared with a 1,4-PDI ethanol solution at $10^{-4}$ M, (B) Ag nanocubes prepared with a 1,4-PDI ethanol solution at $10^{-5}$ M with the number of particles doubled relative to those in part A, and (C) Ag nanocubes prepared by with a 1,4-PDI ethanol solution at $10^{-7}$ M with the number of particles quadrupled relative to those in part A.

Based on the results shown in Figures 2−6, we argue that 4-NTP, 4-ATP, and 1,4-PDI all can readily adsorb onto the surface of Ag nanocubes dispersed in ethanol. To further examine the difference between thiol and isocyanide, we evaluated their competitive adsorption onto the surface of Ag nanocubes by introducing the acid-treated Ag nanocubes into an ethanol solution containing both types of ligands at specific concentrations. Figure 7A shows the Raman spectra collected from an ethanol solution containing 4-NTP and 1,4-PDI (both at $10^{-5}$ M). At $t$ = 3 min, the peaks at 1083, 1336, 1347, and 1572 $cm^{-1}$ could be assigned to $\nu_{CS}$, $\nu_{NO_2}$, and $\nu_{CC}$ of 4-NTP, respectively. However, we could not resolve well-defined peaks associated with 1,4-PDI, except an extremely weak peak located at 2172 $cm^{-1}$. The SERS spectrum remained essentially the same up to $t$ = 60 min. These data confirm that thiol would adsorb onto Ag surface more competitively on the edges of Ag nanocubes where the hot spots are located for SERS detection. Interestingly, when we reduced the 4-NTP concentration by 100-fold to $10^{-7}$ M while keeping the concentration of 1,4-PDI at $10^{-5}$ M, at $t$ = 3 min, Figure 7B shows the appearance of peaks characteristic of 1,4-PDI at 2123 ($\nu_{NC(free)}$) and 2178 $cm^{-1}$ ($\nu_{NC(Ag)}$), together with characteristic peaks of 4-NTP at 1080 ($\nu_{CS}$), 1330 ($\nu_{NO_2}$), and 1568 $cm^{-1}$ ($\nu_{CC}$), We also observed increase in peak intensity for the $\nu_{NC(Ag)}$ band of 1,4-PDI while there was essentially no change to the peaks of 4-NTP by $t$ = 30 min. From $t$ = 30 to 60 min, the SERS spectrum remained unaltered. These results infer that 4-NTP and 1,4-PDI could coexist on the edges of Ag nanocubes.

To further understand the concentration-dependent adsorption of 4-NTP and 1,4-PDI on Ag nanocubes, we repeated the SERS measurements and then analyzed the results. Fitting the $\nu_{CC}$ band of 4-NTP, Figure 8A, shows a plot of the peak area as a function of time by benchmarking against 4-NTP ($10^{-5}$ M). In this case, we noticed that the SERS signal was comparable to that of 4-NTP, suggesting that the 4-NTP could competitively bind to the edges of Ag nanocubes over 1,4-PDI when they were used at the same concentration. On the other hand, when we decreased the concentration of 4-NTP to $10^{-7}$ M while keeping the concentration of 1,4-PDI at $10^{-5}$ M, Figure 8B shows a plot of the $\nu_{CC}$ band of 4-NTP as a function of time by benchmarking against the plot of 4-NTP ($10^{-7}$ M). Under this condition, we observed an increase in the peak area


DOI: 10.1021/acs.jpcc.9b05383
J. Phys. Chem. C 2019, 123, 21571−21580

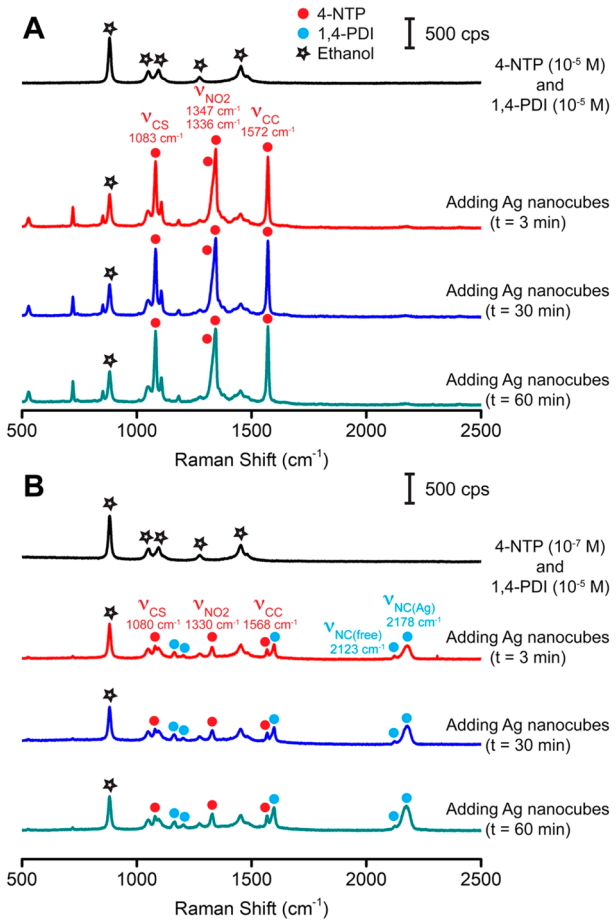


**Figure 7.** (A) Raman spectrum recorded from an ethanol solution containing 4-NTP ($10^{-5}$ M) and 1,4-PDI ($10^{-5}$ M) and the SERS spectra of 4-NTP and 1,4-PDI collected from the same solution at different time points after the introduction of Ag nanocubes. (B) Raman spectrum of an ethanol solution containing 4-NTP ($10^{-7}$ M) and 1,4-PDI ($10^{-5}$ M) and the SERS spectra of 4-NTP and 1,4-PDI collected from the same solution at different time points after adding Ag nanocubes.

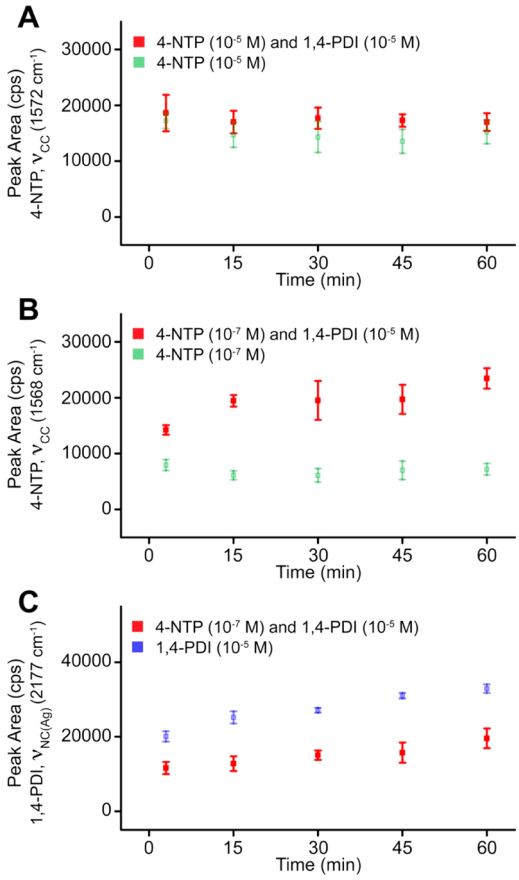


**Figure 8.** (A) Plots of peak area for the $\nu_{CC}$ band of 4-NTP as a function of time when the 4-NTP ($10^{-5}$ M) was mixed with 1,4-PDI ($10^{-5}$ M) by benchmarking against 4-NTP ($10^{-5}$ M). (B) Plots of peak area for the $\nu_{CC}$ band of 4-NTP as a function of time when 4-NTP ($10^{-7}$ M) was mixed with 1,4-PDI ($10^{-5}$ M) by benchmarking against 4-NTP ($10^{-7}$ M). (C) Plots of peak area for the $\nu_{CN(Ag)}$ band of 1,4-PDI as a function of time when 4-NTP ($10^{-7}$ M) was mixed with 1,4-PDI ($10^{-5}$ M) by benchmarking against 1,4-PDI ($10^{-5}$ M).

of 4-NTP when 100-fold more 1,4-PDI molecules were involved in the solution. Because 4-NTP at $10^{-7}$ M was unable to cover the entire surface of Ag nanocubes, we suspect that the adsorption of 1,4-PDI would occur on the side faces of nanocubes, making it possible to favor the preferential adsorption of 4-NTP molecules on the edges of nanocubes for an increase in the SERS signal. Figure 8C shows a plot of the $\nu_{NC(Ag)}$ band of 1,4-PDI as a function of time by benchmarking against the plot of 1,4-PDI ($10^{-5}$ M). Interestingly, we observed a decrease in the SERS signal of 1,4-PDI when a small amount of 4-NTP was involved in the solution. This result indicates that there were fewer number of 1,4-PDI molecules located at the SERS hot spots resulting from the competitive binding of 4-NTP on the edges of nanocubes. Altogether, we argue that it is feasible to use 4-NTP to impede or even inhibit the adsorption of 1,4-PDI molecules on the surface of Ag by maneuvering the concentration of these two ligands.

We also evaluated the competitive adsorption of 4-ATP and 1,4-PDI on Ag using the same experimental approach. Figure 9A shows the Raman spectrum collected from an ethanol solution containing 4-ATP and 1,4-PDI, both at $10^{-5}$ M. At $t$ = 3 min, we observed the peaks of 4-ATP at 1080 ($\nu_{CS}$) and 1595 ($\nu_{CC}$) but not the $\nu_{NC(free)}$ and $\nu_{NC(Ag)}$ bands of 1,4-PDI. Because the $\nu_{CC}$ bands of both1,4-PDI and 4-ATP overlap with each other, we cannot reply on this band for the identification of 1,4-PDI. From $t$ = 30 to 60 min, there was essentially no change to the SERS spectrum. These results are similar to the case of 1,4-PDI and 4-NTP, confirming that thiol binds more strongly to Ag surface than isocyanide regardless of the difference in the terminal group ($NO_2$ vs $NH_2$). Because it was difficult to resolve any SERS signal when decreasing the concentration of 4-ATP from $10^{-5}$ to $10^{-7}$ M (see Figure 4B), we increased the concentration of 1,4-PDI to $10^{-3}$ M while keeping the 4-ATP concentration at $10^{-5}$ M to attain a molar ratio of 4-ATP to 1,4-PDI molecules at 1:100. In this case, at $t$ = 3 min, Figure 9B shows the characteristic peaks of 1,4-PDI at 2125 ($\nu_{NC(free)}$) and 2171 $cm^{-1}$ ($\nu_{NC(Ag)}$) in addition to the peaks of 4-ATP. These results suggest that both 4-ATP and 1,4-PDI could adsorb on the edges of Ag nanocubes at comparable rates when 1,4-PDI was in access, consistent with results of 4-NTP and 1,4-PDI.

## CONCLUSIONS

We have explored the use of in situ SERS to investigate the adsorption of different ligands on the surface of colloidal Ag



DOI: 10.1021/acs.jpcc.9b05383
J. Phys. Chem. C 2019, 123, 21571−21580

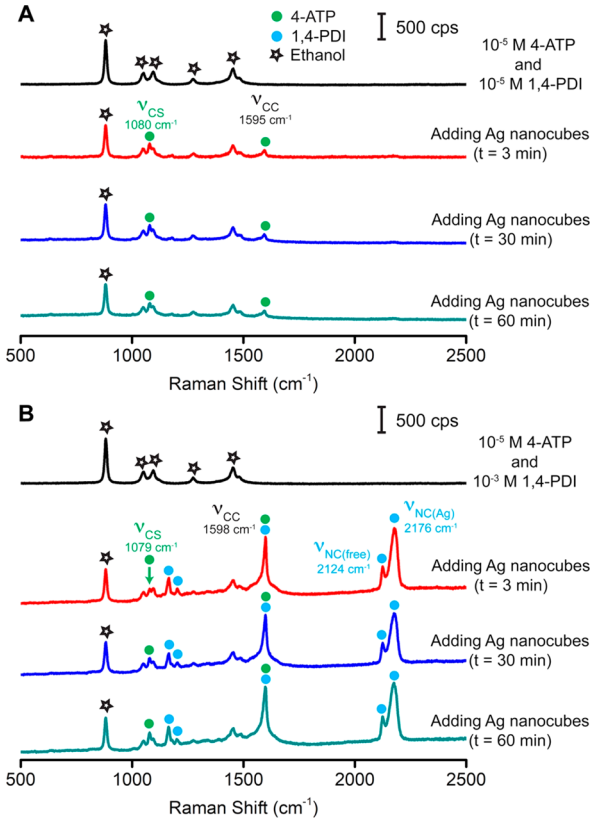


**Figure 9.** (A) Raman spectrum recorded from an ethanol solution containing 4-ATP ($10^{-5}$ M) and 1,4-PDI ($10^{-5}$ M) and the SERS spectra of 4-ATP and 1,4-PDI collected from the same solution at different time points after the introduction of Ag nanocubes. (B) Raman spectrum of an ethanol solution containing 4-ATP ($10^{-5}$ M) and 1,4-PDI ($10^{-3}$ M) and the SERS spectra of 4-ATP and 1,4-PDI collected from the same solution at different time points after adding Ag nanocubes.

nanocubes. In a typical process, we collected SERS spectra at different time points from a mixture of Ag nanocubes and a ligand such as 4-NTP, 4-ATP, or 1,4-PDI at a specific concentration. Time-dependent SERS spectra of 4-NTP indicate that the adsorption could be achieved within 3 min due to the strong binding of thiol to Ag surface. We also recorded the concentration-dependent SERS spectra of 4-NTP, from which we observed a red shift for all peaks at a concentration of $10^{-7}$ M relative to the case of $10^{-5}$ or $10^{-4}$ M. We argue that such a red shift could be attributed to the difference in molecular orientation, with the benzene ring oriented parallel to or tilting away from the surface at low and high concentrations, respectively. We confirmed that the adsorption kinetics of 4-ATP on Ag was similar to that of 4-NTP, although the SERS signals from 4-ATP were much weaker due to the absence of chemical enhancement. Different from the case of thiol, 1,4-PDI would bind to a Ag surface through $\sigma$-donation, giving slower adsorption kinetics over a time scale of 60 min. At a concentration of $10^{-5}$ M and above, we observed both $\nu_{NC(free)}$ and $\nu_{NC(Ag)}$ peaks in the SERS spectra, suggesting that the 1,4-PDI molecules could be oriented with the benzene ring tilting away from the surface. We further evaluated the relative binding strength of the thiol and isocyanide groups toward Ag surface by dispersing Ag nanocubes in an ethanol solution containing both ligands. The SERS signals from 1,4-PDI were not detectable in either case when it was used at the same concentration as 4-NTP or 4-ATP at $10^{-5}$ M. However, the 1,4-PDI signals became detectable when its concentration was increased by 100 times relative to 4-NTP or 4-ATP. Collectively, our data indicate that the thiols have a much stronger binding to the surface on Ag nanocubes, making it possible to impede or even inhibit the adsorption of isocyanides.

## ■ ASSOCIATED CONTENT

### Supporting Information

The Supporting Information is available free of charge on the ACS Publications website at DOI: 10.1021/acs.jpcc.9b05383.

TEM images of Ag nanocubes before and after acid treatment (Figure S1); UV−vis spectra of Ag nanocubes dispersed in acid solution and the as-treated Ag nanocubes redispersed in ethanol (Figure S2); Raman spectra recorded from pure ethanol and ethanol containing as-prepared Ag nanocubes (Figure S3); Raman spectra recorded from 1,4-PDI functionalized Ag nanocubes (Figure S4); and a quantitative summary of the Raman spectra recorded from a reference silicon sample throughout all SERS experiments (Table S1) (PDF)

## ■ AUTHOR INFORMATION


### Corresponding Author

*(D.Q.) E-mail: dong.qin@mse.gatech.edu.

### ORCID

Dong Qin: 0000-0001-5206-5912


### Notes

The authors declare no competing financial interest.

## ■ ACKNOWLEDGMENTS

We acknowledge the support from the National Science Foundation (CHE-1708300) and start-up funds from the Georgia Institute of Technology (GT). The TEM images were obtained using the facilities at the Georgia Tech Institute for Electronics and Nanotechnology, a member of the National Nanotechnology Coordinated Infrastructure (NNCI), which is supported by the National Science Foundation (Grant ECCS-1542174).

## ■ REFERENCES

(1) Gast, A. P.; Adamson, A. W. *Physical chemistry of surfaces*, 6th ed.; Wiley-Interscience: New York, 1997.

(2) Love, J. C.; Estroff, L. A.; Kriebel, J. K.; Nuzzo, R. G.; Whitesides, G. M. Self-Assembled Monolayers of Thiolates on Metals as a Form of Nanotechnology. *Chem. Rev.* **2005**, *105*, 1103−1170.

(3) Templeton, A. C.; Wuelfing, W. P.; Murray, R. W. Monolayer-Protected Cluster Molecules. *Acc. Chem. Res.* **2000**, *33*, 27−36.

(4) Duchesne, L.; Gentili, D.; Comes-Franchini, M.; Fernig, D. G. Robust Ligand Shells for Biological Applications of Gold Nanoparticles. *Langmuir* **2008**, *24*, 13572−13580.

(5) Free, P.; Shaw, C. P.; Lévy, R. PEGylation Modulates the Interfacial Kinetics of Proteases on Peptide-Capped Gold Nanoparticles. *Chem. Commun.* **2009**, 5009−5011.

(6) Nieves, D. J.; Azmi, N. S.; Xu, R.; Lévy, R.; Yates, E. A.; Fernig, D. G. Monovalent Maleimide Functionalization of Gold Nanoparticles via Copper-Free Click Cchemistry. *Chem. Commun.* **2014**, *50*, 13157−13160.

(7) Lévy, R.; Thanh, N. T. K.; Doty, R. C.; Hussain, I.; Nichols, R. J.; Schiffrin, D. J.; Brust, M.; Fernig, D. G. Rational and Combinatorial



DOI: 10.1021/acs.jpcc.9b05383
J. Phys. Chem. C 2019, 123, 21571−21580

Design of Peptide Capping Ligands for Gold Nanoparticles. *J. Am. Chem. Soc.* **2004**, *126*, 10076−10084.
(8) Sperling, R. A.; Rivera Gil, P.; Zhang, F.; Zanella, M.; Parak, W. J. Biological Applications of Gold Nanoparticles. *Chem. Soc. Rev.* **2008**, *37*, 1896−1908.
(9) Daniel, M.-C.; Astruc, D. Gold Nanoparticles: Assembly, Supramolecular Chemistry, Quantum-Size-Related Properties, and Applications Toward Biology, Catalysis, and Nanotechnology. *Chem. Rev.* **2004**, *104*, 293−346.
(10) Badia, A.; Singh, S.; Demers, L.; Cuccia, L.; Brown, G. R.; Lennox, R. B. Self-Assembled Monolayers on Gold Nanoparticles. *Chem. - Eur. J.* **1996**, *2*, 359−363.
(11) Yang, G.; Liu, G.-Y. New Insights for Self-Assembled Monolayers of Organothiols on Au(111) Revealed by Scanning Tunneling Microscopy. *J. Phys. Chem. B* **2003**, *107*, 8746−8759.
(12) Poirier, G. E. Characterization of Organosulfur Molecular Monolayers on Au(111) using Scanning Tunneling Microscopy. *Chem. Rev.* **1997**, *97*, 1117−1128.
(13) Biscarini, F.; Ong, Q. K.; Albonetti, C.; Liscio, F.; Longobardi, M.; Mali, K. S.; Ciesielski, A.; Reguera, J.; Renner, C.; De Feyter, S.; Samorì, P.; Stellacci, F. Quantitative Analysis of Scanning Tunneling Microscopy Images of Mixed-Ligand-Functionalized Nanoparticles. *Langmuir* **2013**, *29*, 13723−13734.
(14) Ong, Q. K.; Reguera, J.; Silva, P. J.; Moglianetti, M.; Harkness, K.; Longobardi, M.; Mali, K. S.; Renner, C.; De Feyter, S.; Stellacci, F. High-Resolution Scanning Tunneling Microscopy Characterization of Mixed Monolayer Protected Gold Nanoparticles. *ACS Nano* **2013**, *7*, 8529−8539.
(15) Stirling, J.; Lekkas, I.; Sweetman, A.; Djuranovic, P.; Guo, Q.; Pauw, B.; Granwehr, J.; Lévy, R.; Moriarty, P. Critical Assessment of the Evidence for Striped Nanoparticles. *PLoS One* **2014**, *9*, No. e108482.
(16) Hostetler, M. J.; Wingate, J. E.; Zhong, C.-J.; Harris, J. E.; Vachet, R. W.; Clark, M. R.; Londono, J. D.; Green, S. J.; Stokes, J. J.; Wignall, G. D.; Glish, G. L.; Porter, M. D.; Evans, N. D.; Murray, R. W. Alkanethiolate Gold Cluster Molecules with Core Diameters from 1.5 to 5.2 nm: Core and Monolayer Properties as a Function of Core Size. *Langmuir* **1998**, *14*, 17−30.
(17) Templeton, A. C.; Hostetler, M. J.; Kraft, C. T.; Murray, R. W. Reactivity of Monolayer-Protected Gold Cluster Molecules: Steric Effects. *J. Am. Chem. Soc.* **1998**, *120*, 1906−1911.
(18) Schneider, L.; Peukert, W. Second Harmonic Generation Spectroscopy as a Method for In Situ and Online Characterization of Particle Surface Properties. *Part. Part. Syst. Charact.* **2006**, *23*, 351−359.
(19) Eisenthal, K. B. Second Harmonic Spectroscopy of Aqueous Nano- and Microparticle Interfaces. *Chem. Rev.* **2006**, *106*, 1462−1477.
(20) Gan, W.; Gonella, G.; Zhang, M.; Dai, H.-L. Communication: Reactions and Adsorption at the Surface of Silver Nanoparticles Probed by Second Harmonic Generation. *J. Chem. Phys.* **2011**, *134*, No. 041104.
(21) Campen, R. K.; Zheng, D.-S.; Wang, H.-F.; Borguet, E. Second Harmonic Generation as a Probe of Multisite Adsorption at Solid−Liquid Interfaces of Aqueous Colloid Suspensions. *J. Phys. Chem. C* **2007**, *111*, 8805−8813.
(22) Dinkel, R.; Braunschweig, B.; Peukert, W. Fast and Slow Ligand Exchange at the Surface of Colloidal Gold Nanoparticles. *J. Phys. Chem. C* **2016**, *120*, 1673−1682.
(23) Weaver, M. J. Raman and Infrared Spectroscopies as In Situ probes of Catalytic Adsorbate Chemistry at Electrochemical and Related Metal−Gas Interfaces: Some Perspectives and Prospects. *Top. Catal.* **1999**, *8*, 65−73.
(24) Weaver, M. J. Surface-Enhanced Raman Spectroscopy as a Versatile In Situ Probe of Chemisorption in Catalytic Electrochemical and Gaseous Environments. *J. Raman Spectrosc.* **2002**, *33*, 309−317.
(25) Tian, Z. Q.; Ren, B. Adsorption and Reaction at Electrochemical Interfaces as Probed by Surface-Enhanced Raman Spectroscopy. *Annu. Rev. Phys. Chem.* **2004**, *55*, 197−229.
(26) Fokas, C.; Deckert, V. Towards In Situ Raman Microscopy of Single Catalytic Sites. *Appl. Spectrosc.* **2002**, *56*, 192−199.
(27) Gomez, R.; Solla-Gullon, J.; Perez, J. M.; Aldaz, A. Nanoparticles-on-Electrode Approach for *In Situ* Surface-Enhanced Raman Spectroscopy Studies with Platinum-Group Metals: Examples and Prospects. *J. Raman Spectrosc.* **2005**, *36*, 613−622.
(28) Zhang, Y.; Wu, Y.; Qin, D. Rational Design and Synthesis of Bifunctional Metal Nanocrystals for Probing Catalytic Reactions by Surface-Enhanced Raman Scattering. *J. Mater. Chem. C* **2018**, *6*, 5353−5362.
(29) Huang, J.; Zhu, Y.; Lin, M.; Wang, Q.; Zhao, L.; Yang, Y.; Yao, K. X.; Han, Y. Site-Specific Growth of Au−Pd Alloy Horns on Au Nanorods: A Platform for Highly Sensitive Monitoring of Catalytic Reactions by Surface Enhancement Raman Spectroscopy. *J. Am. Chem. Soc.* **2013**, *135*, 8552−8561.
(30) Li, J.; Wu, Y.; Sun, X.; Liu, J.; Winget, S. A.; Qin, D. A Dual Catalyst with SERS Activity for Probing Stepwise Reduction and Oxidation Reactions. *ChemNanoMat* **2016**, *2*, 786−790.
(31) Zhang, Y.; Liu, J.; Ahn, J.; Xiao, T.-H.; Li, Z.-Y.; Qin, D. Observing the Overgrowth of a Second Metal on Silver Cubic Seeds in Solution by Surface-Enhanced Raman Scattering. *ACS Nano* **2017**, *11*, 5080−5086.
(32) Wu, Y.; Qin, D. In Situ Atomic-Level Tracking of Heterogeneous Nucleation in Nanocrystal Growth with an Isocyanide Molecular Probe. *J. Am. Chem. Soc.* **2018**, *140*, 8340−8349.
(33) Muniz-Miranda, M.; Pagliai, M.; Cardini, G.; Schettino, V. Role of Surface Metal Clusters in SERS Spectra of Ligands Adsorbed on Ag Colloidal Nanoparticles. *J. Phys. Chem. C* **2008**, *112*, 762−767.
(34) Zhang, D.; Ansar, S. M. Ratiometric Surface Enhanced Raman Quantification of Ligand Adsorption onto a Gold Nanoparticle. *Anal. Chem.* **2010**, *82*, 5910−5914.
(35) Darby, B. L.; Le Ru, E. C. Competition between Molecular Adsorption and Diffusion: Dramatic Consequences for SERS in Colloidal Solutions. *J. Am. Chem. Soc.* **2014**, *136*, 10965−10973.
(36) Futamata, M. Surface-Plasmon-Polariton-Enhanced Raman Scattering from Self-Assembled Monolayers of p-Nitrothiophenol and p-Aminothiophenol on Silver. *J. Phys. Chem.* **1995**, *99*, 11901−11908.
(37) Walczak, M. M.; Chung, C.; Stole, S. M.; Widrig, C. A.; Porter, M. D. Structure and Interfacial Properties of Spontaneously Adsorbed n-Alkanethiolate Monolayers on Evaporated Silver Surfaces. *J. Am. Chem. Soc.* **1991**, *113*, 2370−2378.
(38) Kim, K.; Choi, J.-Y.; Shin, K. S. Surface-Enhanced Raman Scattering of 4-Nitrobenzenethiol and 4-Aminobenzenethiol on Silver in Icy Environments at Liquid Nitrogen Temperature. *J. Phys. Chem. C* **2014**, *118*, 11397−11403.
(39) Zhao, L.-B.; Chen, J.-L.; Zhang, M.; Wu, D.-Y.; Tian, Z.-Q. Theoretical Study on Electroreduction of p-Nitrothiophenol on Silver and Gold Electrode Surfaces. *J. Phys. Chem. C* **2015**, *119*, 4949−4958.
(40) Fang, Y.; Li, Y.; Xu, H.; Sun, M. Ascertaining p,p'-Dimercaptoazobenzene Produced from p-Aminothiophenol by Selective Catalytic Coupling Reaction on Silver Nanoparticles. *Langmuir* **2010**, *26*, 7737−7746.
(41) Zhang, J.; Winget, S. A.; Wu, Y.; Su, D.; Sun, X.; Xie, Z.-X.; Qin, D. Ag@Au Concave Cuboctahedra: A Unique Probe for Monitoring Au-Catalyzed Reduction and Oxidation Reactions by Surface-Enhanced Raman Spectroscopy. *ACS Nano* **2016**, *10*, 2607−2616.
(42) Gajdo, M.; Eichler, A.; Hafner, J. CO Adsorption on Close-packed Transition and Noble Metal Surfaces: Trends From *Ab Initio* Calculations. *J. Phys.: Condens. Matter* **2004**, *16*, 1141−1164.
(43) Gruenbaum, S. M.; Henney, M. H.; Kumar, S.; Zou, S. Surface-Enhanced Raman Spectroscopic Study of 1,4-Phenylene Diisocyanide Adsorbed on Gold and Platinum-Group Transition Metal Electrodes. *J. Phys. Chem. B* **2006**, *110*, 4782−4792.
(44) Bae, S. J.; Lee, C.-R.; Choi, I. S.; Hwang, C.-S.; Gong, M.-S.; Kim, K.; Joo, S.-W. Adsorption of 4-Biphenylisocyanide on Gold and Silver Nanoparticle Surfaces: Surface-Enhanced Raman Scattering Study. *J. Phys. Chem. B* **2002**, *106*, 7076−7080.


DOI: 10.1021/acs.jpcc.9b05383
*J. Phys. Chem. C* 2019, 123, 21571−21580

(45) Hu, J.; Tanabe, M.; Sato, J.; Uosaki, K.; Ikeda, K. Effects of Atomic Geometry and Electronic Structure of Platinum Surfaces on Molecular Adsorbates Studied by Gap-Mode SERS. *J. Am. Chem. Soc.* **2014**, *136*, 10299−10307.
(46) Han, H. S.; Han, S. W.; Joo, S. W.; Kim, K. Adsorption of 1,4-Phenylene Diisocyanide on Silver Investigated by Infrared and Raman Spectroscopy. *Langmuir* **1999**, *15*, 6868−6874.
(47) Angelici, R. J.; Lazar, M. Isocyanide Ligands Adsorbed on Metal Surfaces: Applications in Catalysis, Nanochemistry, and Molecular Electronics. *Inorg. Chem.* **2008**, *47*, 9155−9165.
(48) Sato, S.; Iwase, S.; Namba, K.; Ono, T.; Hara, K.; Fukuoka, A.; Uosaki, K.; Ikeda, K. Electrical Matching at Metal/Molecule Contacts for Efficient Heterogeneous Charge Transfer. *ACS Nano* **2018**, *12*, 1228−1235.
(49) Skrabalak, S. E.; Au, L.; Li, X.; Xia, Y. Facile Synthesis of Ag Nanocubes and Au Nanocages. *Nat. Protoc.* **2007**, *2*, 2182−2190.
(50) Li, J.; Liu, J.; Yang, Y.; Qin, D. Bifunctional Ag@Pd-Ag Nanocubes for Highly Sensitive Monitoring of Catalytic Reactions by Surface-Enhanced Raman Spectroscopy. *J. Am. Chem. Soc.* **2015**, *137*, 7039−7042.
(51) Matsuura, T.; Shimoyama, Y. Growth Kinetics of Self-Assembled Monolayers of Thiophene and Terthiophene on Au(111): An Infrared Spectroscopic Study. *Eur. Phys. J. E: Soft Matter Biol. Phys.* **2002**, *7*, 233−240.
(52) Xu, S.; Cruchon-Dupeyrat, S. J. N.; Garno, J. C.; Liu, G.-Y.; Jennings, G. K.; Yong, T.-H.; Laibinis, P. E. *In Situ* Studies of Thiol Self-Assembly on Gold from Solution Using Atomic Force Microscopy. *J. Chem. Phys.* **1998**, *108*, 5002−5012.
(53) Jakubowicz, A.; Jia, H.; Wallace, R. M.; Gnade, B. E. Adsorption Kinetics of p-Nitrobenzenethiol Self-Assembled Monolayers on a Gold Surface. *Langmuir* **2005**, *21*, 950−955.



DOI: 10.1021/acs.jpcc.9b05383
*J. Phys. Chem. C* 2019, 123, 21571−21580